

# Energy Transfer Between the Flavin Chromophores of Electron-Transferring Flavoprotein from *Megasphaera elsdenii* as Inferred from Time-Resolved Red-Edge and Blue-Edge Fluorescence Spectroscopy

P. I. H. Bastiaens,<sup>1</sup> S. G. Mayhew,<sup>2</sup> E. M. O'Nualláin,<sup>2,3</sup> A. van Hoek,<sup>1</sup> and A. J. W. G. Visser<sup>1,4</sup>

Received March 13, 1991; revised June 27, 1991; accepted June 28, 1991

Both a mode-locked argon-ion laser and synchrotron radiation were used as excitation sources to obtain time-resolved polarized fluorescence of the two FAD cofactors in electron transferring flavoprotein from *Megasphaera elsdenii*. Red-edge excited and blue-edge detected fluorescence anisotropy decay curves did not contain a fast relaxation process which was observed upon main-band excitation and detection. This relaxation was assigned to homo-energy transfer between the two FAD cofactors. Failure of energy transfer as observed with edge spectroscopy on this protein excludes restricted reorientational motion of the flavins as a possible mechanism of depolarization. From the global analysis of the fluorescence anisotropy decay surface obtained at multiple excitation and detection wavelengths, the distance between and the relative orientation of the flavins could be estimated. The methodology described has general applicability in other multichromophoric biopolymers and has the potential to acquire accurate geometrical parameters in these systems.

**KEY WORDS:** Homo-energy transfer; flavin; red edge; blue edge; fluorescence anisotropy.

## INTRODUCTION

The electron transferring flavoprotein (ETF) from *Megasphaera elsdenii* functions in the formation of short-chain fatty acids by coupling the oxidation of NADH or D-lactate dehydrogenase to the reduction of butyryl-CoA dehydrogenase [1]. ETF from *Megasphaera elsdenii* is unusual in comparison to ETF isolated from mammalian and other bacterial sources in that it contains two highly fluorescent noncovalently bound FAD cofactors (quan-

tum yield is 2.4 that of free FAD) instead of one per protein molecule [2]. The 74-kDa protein has a  $\alpha\beta$  ( $\alpha$ , 41 kDa;  $\beta$ , 33 kDa) dimeric quaternary structure with the two FAD cofactors residing on the  $\beta$  subunit. No information is available on the spatial relationship of the FAD cofactors within the protein. One of the techniques to obtain insight in this spatial relationship is to monitor the fluorescence resonance energy transfer (FRET) between the isoalloxazinic residues of the FAD cofactors in a time-resolved fluorescence anisotropy experiment. Energy transfer between like chromophores, termed homo-transfer, cannot be observed in the decay of the fluorescence since this process does not affect the lifetime of the excited state. Instead, the relaxation of the excited state by dipole-dipole coupling in a homo-transfer system can be observed in the depolarization of the fluorescence when the directions of the transition moments

<sup>1</sup> Department of Biochemistry, Agricultural University, 6703HA Wageningen, The Netherlands.

<sup>2</sup> Department of Biochemistry, University College Dublin, Belfield, Dublin 4, Ireland.

<sup>3</sup> Present address: Research Centre, Our Lady's Hospital for Sick Children, Dublin, Ireland.

<sup>4</sup> To whom correspondence should be addressed.

do not coincide in the interacting moieties [3–5]. The rate of transfer can be obtained from the relaxation of the fluorescence anisotropy in a time-resolved experiment [3, 6]. The distance between the chromophores can be estimated with the Förster relation [7] given that the geometric parameter  $\kappa^2$  and the overlap integral  $J$  are known.  $J$  can be determined from the overlap between absorption and fluorescence emission spectra of the chromophores in question. The exact value of the geometric factor  $\kappa^2$  is hard to obtain, if not impossible, in certain circumstances. Dale *et al.* [8] presented contour plots to estimate upper and lower boundaries of  $\kappa^2$  provided that restricted reorientational motion of interacting chromophores takes place on a frequency scale which is much larger than the transfer rate (dynamic averaging regime). The axial depolarization due to restricted motion of the individual chromophores must be known for an estimate of  $\kappa^2$ . In a completely rigid system with one unique configuration of the interacting chromophores, one cannot obtain information on  $\kappa^2$  from a fluorescence experiment. Only an upper limit can be assigned to  $\kappa^2$ , leading to an upper limit of the distance between the chromophores [8].

One of the complications associated with the measurement of homo-transfer by fluorescence anisotropy is that the depolarization of the fluorescence can arise not only from energy transfer, but also from restricted reorientational motion of the chromophores inside the protein. One solution to solve this ambiguity in the interpretation of the fluorescence anisotropy is to alter the system in a biochemical fashion by selectively removing one of the covalently bound chromophores and comparing the anisotropy of this partial apo-protein with that of the holo-protein. In practice this is difficult to achieve, especially when the active sites are similar, with comparable dissociation constants of the cofactors. Another problem is that the dynamical behavior of the chromophores inside the protein can be influenced by removal of one of them [5]. The other, physical solution is to excite the sample at the red edge of the absorption band and monitoring the resulting decay of fluorescence anisotropy. In a system where the fluorescence depolarization is caused by homo-transfer, red-edge excitation in the absorption band will decrease the probability of transfer, with a corresponding decrease in the transfer rate [5,9–12]. Extreme edge excitation will result in complete failure of energy as observed in aromatic fluorophores in viscous polar media at low temperatures [13, 14]. This phenomenon will take place only in a system with inhomogeneously broadened fluorescence spectra and long dipolar relaxation time in comparison to the fluorescence lifetime [9–11, 15]. Such a situation may correspond to a chromophore in a polar protein environment where

dynamical events take place on a time scale which is much longer than the fluorescence lifetime.

As energy transfer is directed from “blue” (large 0-0 energy separation) to “red” (small 0-0 energy separation) centers [11], a phenomenon similar to red-edge failure of energy transfer is expected upon detection at the blue edge of the emission band. Photons which are emitted at the blue edge of the emission have the largest energy and must therefore originate from chromophores which did not participate in energy transfer. Photons which originate from chromophores involved in energy transfer will have a lower polarization than photons from nontransferring chromophores. Both red-edge and blue-edge failure of energy transfer will be manifest in the anisotropy decay by an increase in the relaxation time constant associated with energy transfer and an increase in the fluorescence anisotropy.

To ascertain that energy transfer takes place between the FAD cofactors, we used both a synchrotron and a mode-locked argon-ion laser as excitation sources in order to perform a variable wavelength and time-resolved fluorescence experiment. The advantage of the former source is the continuous tunability of the excitation wavelength, with the disadvantage of the lower intensity and larger frequency bandwidth in comparison to the latter excitation source. The argon-ion laser contains two excitation wavelengths, which correspond to the main band (457.9 nm) and red edge (514.5 nm) of the normal flavin absorption spectrum. Therefore this pulsed excitation source is suitable to perform flavin red-edge spectroscopy. The narrow bandwidth in the case of the 514.5-nm line (5-GHz bandwidth) enables highly selective excitation of nonequilibrium solvates at the red edge of the absorption band [15].

Multiple fluorescence anisotropy decays of ETF have been collected as a function of excitation and detection wavelengths. This set of curves can be combined to form a fluorescence anisotropy decay surface. Global analysis of this data surface to a single model by exploiting the relations between the parameters of the different experiments allows for better model discrimination by statistical criteria and parameter recovery than single-curve analysis of individual experiments [16–18].

## MATERIALS AND METHODS

### Biochemical Manipulation

ETF was purified from *Megasphaera elsdenii* [2], and stored at 4°C as a precipitate of ammonium sulfate (80% saturation). Prior to an experiment, the precipitate

was dissolved in 50 mM  $KP_i$ , pH 6.0, and 0.3 mM EDTA, and the solution chromatographed on a column of Bio-Gel PDG-6 (Bio-Rad) equilibrated with the same buffer to remove any protein-free FAD. The preparation was judged to be homogeneous by polyacrylamide gel electrophoresis (PAGE) in the presence and absence of sodium dodecyl sulfate (SDS). It was used as isolated, without addition of FAD to saturate the flavin sites [2]. The visible absorption spectrum of the preparation showed that it contained a slight contamination of 8-OH-FAD [19], not exceeding 5% of the total FAD.

### Steady-State Spectra

Absorption spectra was recorded on a Cary 17 spectrophotometer and fluorescence emission spectra on an Aminco SPF-500 fluorimeter.

### Time-Resolved Fluorometry

Time-correlated single photon counting (TCSPC) was used as the technique to measure fluorescence and fluorescence anisotropy decays [20]. For excitation with 457.9- and 514.5-nm light, a mode-locked cw argon-ion laser was used (Coherent Radiation model CR-18). The pulses were about 100 ps FWHM with picjoule energies after the excitation rate was diminished from 76 MHz to 596 kHz by an electrooptic modulator [21]. The fluorescence was collected at 90° with respect to the direction of the exciting light beam. Between the sample and the microchannel plate detector (Hamamatsu 1645-U), filters were placed to select blue-edge (Schott KV 500 + Balzers 501), main-band (Schott OG 530 + Schott 539.4), and red-edge (Schott KV 500 + Schott 568.5) portions of the flavin emission. Parallel- and perpendicular-polarized fluorescence intensities were collected with a computer controlled rotatable sheet polarizer (Polaroid HN38). The sequence of data acquisition consisted of 10 cycles of 10-s collection of parallel- and perpendicular-polarized sample fluorescence sandwiched between the collection of two cycles of 10 s of parallel and perpendicular pulse mimic (erythrosin B in water). The detection count rate was set at 30 kHz in the parallel-polarized detection to prevent pulse pile-up distortion of the data. Background fluorescence was sampled at one-fifth of the sample acquisition time and was always below 1% of the sample count rate. Details of the experimental setup and detection electronics are presented elsewhere [12]. The data were transferred from the multichannel analyzer to a MicroVax station for data analysis.

For excitation at 435, 445, 451, and 515 nm, the

synchrotron radiation facility at Daresbury, UK, was used [22]. The excitation wavelength was selected with a double monochromator, with the slit width set at 1.5 nm. Detection wavelengths were selected by placing interference filters (Ealing, 10-nm bandpass) between the sample and the microchannel plate detector (Hamamatsu R-1564-U). Parallel- and perpendicular-polarized emission intensities were collected by sampling 1 cycle of 100 s of parallel and perpendicular fluorescence each. The pulse was acquired by placing a scatterer (Ludox in water) in the sample housing and tuning the excitation wavelength at the maximal transmission of the interference filter in use. The pulse was sampled in the parallel position of the polarizer until 20,000 counts in the peak were obtained. Background fluorescence of the buffer solution of ETF was, in all cases, negligible.

### Data Analysis

The fluorescence anisotropy data surface was analyzed with a version especially designed for TCSPC data of the commercially available global analysis program (Globals Unlimited, Urbana IL) based on the iterative reconvolution method [18]. The total fluorescence decays were constructed from parallel- and perpendicular-polarized intensity decay files with the background subtracted and proper weighting applied [23]. For the deconvolution of the fluorescence decays obtained from laser excitation, the reference method was used with erythrosin B in water as a reference compound ( $\tau_{ref} = 80$  ps) [23]. For the deconvolution of the fluorescence decays obtained with the synchrotron radiation source, the pulse as acquired with a scatterer was used. The fluorescence decays of ETF were fitted to a triple-exponential function to obtain  $\chi^2$  values close to unity. This method does not give any insight into the physical process underlying the fluorescence decay but allows for the analysis of the anisotropy decay surface. The optimized parameters of the fluorescence decays were fixed in the subsequent analysis of the fluorescence anisotropy decays obtained at different excitation and emission wavelengths were simultaneously fitted to a model described under Results. All parameters of the parallel- and perpendicular-polarized fluorescence intensity components of individual experiments were linked [18]. The fit of the data surface was subjected to rigorous error analysis to yield an estimate of the standard error of the anisotropy decay parameters [18].

## RESULTS

### Fluorescence Decay

In Table I the parameters of the triple-exponential fit ( $\chi^2$  close to 1) of the fluorescence decays of ETF excited and detected at different wavelengths are gathered. The nonhomogeneous fluorescence decay is often observed for intrinsic fluorophores in proteins and reflects the inhomogeneity of the chromophore environment. No effort was made to interpret the observed nonhomogeneous fluorescence decay in a quantitative fashion as our attention was directed to the spatial relationships of the FADs as contained in the fluorescence anisotropy decay. The fluorescence decay parameters as listed in Table I were fixed in the analysis of the fluorescence anisotropy decay surface.

### Fluorescence Anisotropy Decay

Let us assume as a working hypothesis that the depolarization of the flavin fluorescence in ETF is caused by (i) homo-transfer between the FAD cofactors and (ii) protein tumbling. The model describing the anisotropy decay  $r(t)$  is then given by [3, 5]

$$r(t) = \{\beta_1 \exp(-t/\phi_T) + \beta_2\} \exp(-t/\phi_P) \quad (1)$$

where  $\phi_P$  is the correlation time of protein tumbling related to the molecular volume ( $V$ ) of the protein and viscosity of the solvent ( $\eta$ ) by the Stokes-Einstein re-

lation, assuming that the protein is spherical and much larger than the solvent molecules. The transfer correlation time  $\phi_T$  is directly related to the rate of energy transfer  $k_T$  [4-6]:

$$\phi_T = \frac{1}{2k_T} \quad (2)$$

The amplitudes  $\beta_1$  and  $\beta_2$  contain geometrical information on intra- and intermolecular angles of absorption and emission transition moments of the interacting moieties [3, 4]:

$$\beta_1 = \frac{1}{10} [2P_2(\mathbf{u}_a^1 \cdot \mathbf{u}_c^1) - P_2(\mathbf{u}_a^1 \cdot \mathbf{u}_c^2) - P_2(\mathbf{u}_a^2 \cdot \mathbf{u}_c^1)] \quad (3)$$

$$\beta_2 = \frac{1}{10} [2P_2(\mathbf{u}_a^1 \cdot \mathbf{u}_c^1) + P_2(\mathbf{u}_a^1 \cdot \mathbf{u}_c^2) + P_2(\mathbf{u}_a^2 \cdot \mathbf{u}_c^1)] \quad (4)$$

where  $P_2(\mathbf{u}_a^i \cdot \mathbf{u}_c^j)$  is the second-order Legendre polynomial of the vector product of the transition moment of absorption  $\mathbf{u}_a^i$  in molecule  $i$ , and transition moment of emission  $\mathbf{u}_c^j$  in molecule  $j$ . When  $i=j$  the vector product is a function of the intramolecular angle of absorption and emission in a chromophore, whereas when  $i \neq j$  it is a function of the intermolecular angle of absorption and emission transition moments of the interacting chromophores.

Since the amplitudes are dependent only on the relative positions of the transition moments of the chromophores in the protein, they should be physical invariants of excitation and detection wavelengths as long as the first electronic transition is excited. Consequently, the amplitudes can be linked in the fit of the anisotropy data surface as obtained by variation of excitation and emission wavelengths. The correlation time of protein tumbling is also independent of excitation or detection wavelengths and is thus also an overdetermined parameter in the fit of the data surface [25].

The probability of energy transfer is strongly dependent on the excitation and emission wavelengths. Upon excitation at the red edge of the absorption or detection at the blue edge of the emission, the rate of transfer should approach zero if, indeed, failure of energy transfer occurs in the system under investigation. The corresponding transfer correlation time should then approach infinity. The observation of these phenomena provides strong indications that the depolarization of the fluorescence upon main-band excitation and detection is caused by homo-energy transfer.

Table I. Fluorescence Decay Parameters of ETF

Excitation and detection wavelength		Parameter <sup>c</sup>					
$\lambda_{\text{ex}}$ (nm) <sup>a</sup>	$\lambda_{\text{em}}$ (nm) <sup>b</sup>	$\alpha_1$	$\alpha_2$	$\alpha_3$	$\tau_1$ (ns)	$\tau_2$ (ns)	$\tau_3$ (ns)
435 (S)	460	0.64	0.28	0.08	0.086	0.70	2.29
445 (S)	470	0.63	0.28	0.09	0.11	0.61	1.83
458 (L)	501	0.53	0.40	0.07	0.33	1.35	3.20
458 (L)	539	0.41	0.53	0.06	0.43	1.34	3.26
458 (L)	569	0.30	0.65	0.05	0.66	1.37	3.53
515 (L)	548	0.10	0.84	0.06	0.61	1.16	2.90

<sup>a</sup>Excitation wavelength in nanometers, where S denotes synchrotron and L denotes laser as excitation source.

<sup>b</sup>Maximum transmission of interference filter used, where the bandwidth at half-maximum transmission was approximately 10 nm for all filters.

<sup>c</sup>All fluorescence decays were fitted to a triple-exponential function:

$$I(t) = \sum_{i=1}^3 \alpha_i \exp(-t/\tau_i).$$

In our global analysis of the experiments, we have chosen not to include overlapping experiments obtained with the two excitation sources. We omitted the polarized decay curves arising from 450- and 515-nm synchrotron excitation. This was done because the quality of the data was not as good as that obtained with laser excitation, due to radiofrequency interference and detection of some white scattered light. In order to show the good reproducibility, however, we included the results of a separate analysis of experiments with synchrotron excitation at 450 and 515 nm (*vide infra*).

In Table II the global link matrix as used in the analysis of the data according to Eq. (1) is presented. One dimension represents the type of experiment (change of excitation and/or emission wavelength), and the other dimension the parameters of the model. Parameters which are linked have the same logic number in different experiments [18]. In Fig. 1 the absorption and emission spectra of ETF are shown with arrows marking the used excitation and emission wavelengths. From Fig. 1 it can be seen that a substantial overlap exists between the two spectra. Energy transfer may then be possible between both FAD cofactors.

The anisotropy data surface of ETF was fitted to Eq. (1) with the linkage between parameters of different decays presented in Table II. The parameters are collected in Table III together with the standard errors as estimated from a rigorous error analysis (67% confidence interval). Fitting criteria, such as the residuals and local and global  $\chi^2$  values [26] are presented in Fig. 2. This figure demonstrates that an optimized fit was achieved.

Table II. Global Link Matrix

Excitation and detection wavelength		Parameter <sup>c</sup>			
$\lambda_{\text{ex}}$ (nm) <sup>a</sup>	$\lambda_{\text{em}}$ (nm) <sup>b</sup>	$\beta_1$	$\beta_2$	$\phi_p$	$\phi_T$
435 (S)	460	1	2	3	4
445 (S)	470	1	2	3	5
458 (L)	501	1	2	3	6
458 (L)	539	1	2	3	7
458 (L)	569	1	2	3	8
515 (L)	548	1	2	3	9

<sup>a</sup>Excitation wavelength in nanometers, where S denotes synchrotron and L denotes laser as excitation source.

<sup>b</sup>Maximum transmission of interference filter used, where the bandwidth at half-maximum transmission was approximately 10 nm for all filters.

<sup>c</sup>Parameters of Eq. 1 (see text).

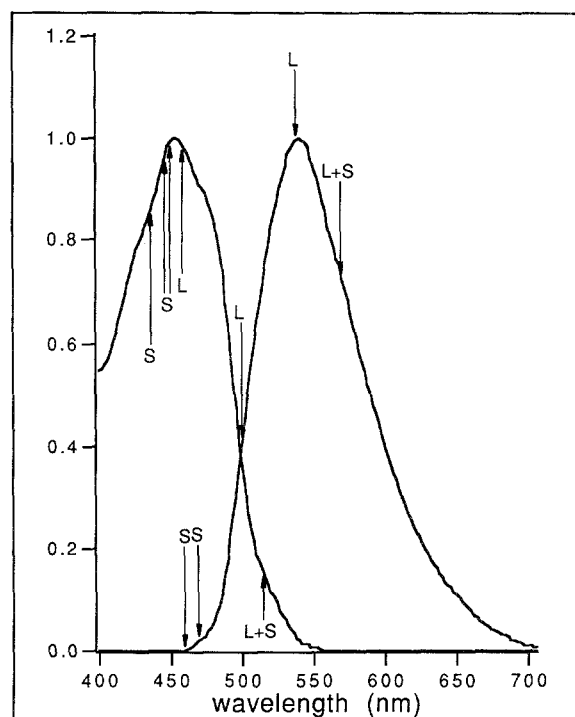


Fig. 1. Absorption and emission spectra of electron transferring flavoprotein. Arrows on the absorption spectrum (pointing upward) indicate the excitation wavelengths and source (S, synchrotron; L, laser). Arrows on the emission spectrum (pointing downward) indicate the detection wavelengths used.

A global analysis with a linking scheme analogous to that in Table II was performed on the data originating from synchrotron excitation at 450 and 515 nm. The results are displayed and collected in Fig. 3 and Table IV, respectively. It can be concluded that excellent agreement exists between the anisotropy decay parameters as obtained for both synchrotron and laser excitation at similar wavelength settings. It is also to be noted that different batches of protein were used.

From Tables III and IV and Fig. 3, it can be concluded that a fast process is present in the anisotropy decay upon main-band (435- to 460-nm) excitation and detection between 530 and 570 nm. This process becomes slower, as apparent from an increase in correlation time upon blue-edge (501-nm) detection and vanishes completely at the extreme blue edge (460–470 nm). Upon red-edge (515-nm) excitation, a completely analogous situation is encountered. Both extreme blue-edge detection and red-edge excitation thus abolish a process observed at main-band excitation and detection. This process must then be ascribed to homo-energy transfer between the FAD cofactors.

Table III. Fluorescence Anisotropy Decay Parameters of ETF

Excitation and detection wavelength		Value of parameter <sup>c</sup>			
$\lambda_{\text{ex}}$ (nm) <sup>a</sup>	$\lambda_{\text{em}}$ (nm) <sup>b</sup>	$\beta_1$	$\beta_2$	$\phi_p$ (ns)	$\phi_T$ (ns)
435 (S)	460	0.0556 (0.0491–0.0645)	0.298 (0.288–0.304)	14.5 (13.0–16.7)	$45 \cdot 10^3$
445 (S)	470	"	"	"	$18 \cdot 10^4$
458 (L)	501	"	"	"	1.71 (1.16–2.60)
458 (L)	539	"	"	"	0.437 (0.250–0.706)
458 (L)	569	"	"	"	0.171 (0.0773–0.317)
515 (L)	548	"	"	"	51.9

<sup>a</sup>Excitation wavelength in nanometers, where S denotes synchrotron and L denotes laser as excitation source.

<sup>b</sup>Maximum transmission of interference filter used where the bandwidth at half-maximum transmission was approximately 10 nm for all filters.

<sup>c</sup>Parameters of Eq. (1) (see text), with standard errors (at 67% confidence level) in parentheses, as obtained from a rigorous error analysis.

From the preexponential amplitudes of Eq. (1) this inter- and intramolecular angles between absorption and emission moments can be estimated. Addition of Eqs. (3) and (4) yields the value of the fundamental anisotropy:

$$\beta_1 + \beta_2 = \frac{2}{5} P_2[\mathbf{u}_a^1 \cdot \mathbf{u}_e^1] \quad (5)$$

From Eq. (5) the intramolecular angle of the transition moments in the isoalloxazinic ring of the FAD cofactors can be calculated. With the values of  $\beta_1$  and  $\beta_2$  as obtained from the global analysis (Table II), we obtained an angle  $\delta$  of  $16 \pm 2^\circ$ .

Upon subtraction of Eq. (4) from Eq. (3) we obtain

$$\beta_2 - \beta_1 = \frac{1}{5} P_2[\mathbf{u}_a^1 \cdot \mathbf{u}_e^2] + \frac{1}{5} P_2[\mathbf{u}_a^2 \cdot \mathbf{u}_e^1] \quad (6)$$

The two second-order Legendre polynomials on the right-hand side of Eq. (6) can, in principle, not be solved except when they are equal ( $\delta=0$ ). This situation corresponds to equal intermolecular angles of absorption and emission transition dipoles in both possible directions of energy transfer. In the isoalloxazines of FAD there are two possible cases. Either the angle  $\delta$  is not equal to zero or there exists extremely fast restricted reorientation of the flavins which cannot be resolved by our TCSPC apparatus. An estimation of the intermolec-

ular angle of absorption and emission transition moments can be made by assuming that the angles are equal in both directions of energy transfer. From the average Legendre polynomial as obtained by subtraction of the preexponential amplitudes [Eq. (6)], we can then calculate an angle  $\epsilon$  of  $31 \pm 2^\circ$ .

From red-edge excitation and blue-edge detected anisotropy experiments, no depolarization process other than protein tumbling on a time scale comparable to that of the fluorescence emission was apparent. The value for the initial anisotropy is lower than the fundamental one of 0.4, which could originate from picosecond restricted motion. Alternatively, as outlined above, the intramolecular angle between absorption and emission transition moments is not zero. In the latter case the flavins are completely immobilized in the protein and the geometrical factor  $\kappa^2$  of the Förster equation cannot be estimated. The only remedy is then to assign an upper limit of 4 to this parameter [8] to calculate a maximal possible distance between the isoalloxazinic residues of the FAD cofactors in ETF. From the transfer correlation time obtained at main-band excitation and detection, we calculated a transfer rate  $k_T$  of  $2.93 \text{ ns}^{-1}$ . With the overlap integral as determined from the absorption and emission spectra in Fig. 1 ( $J = 5.53 \cdot 10^{-15} \text{ M}^{-1} \text{ cm}^3$ ), the radiative rate of isoalloxazine ( $\lambda_r = 0.0556 \text{ ns}^{-1}$ ) [27] and the refractive index ( $n = 1.4$ ) [28], we calculated from the Förster equation [7, 29] an upper limit for the

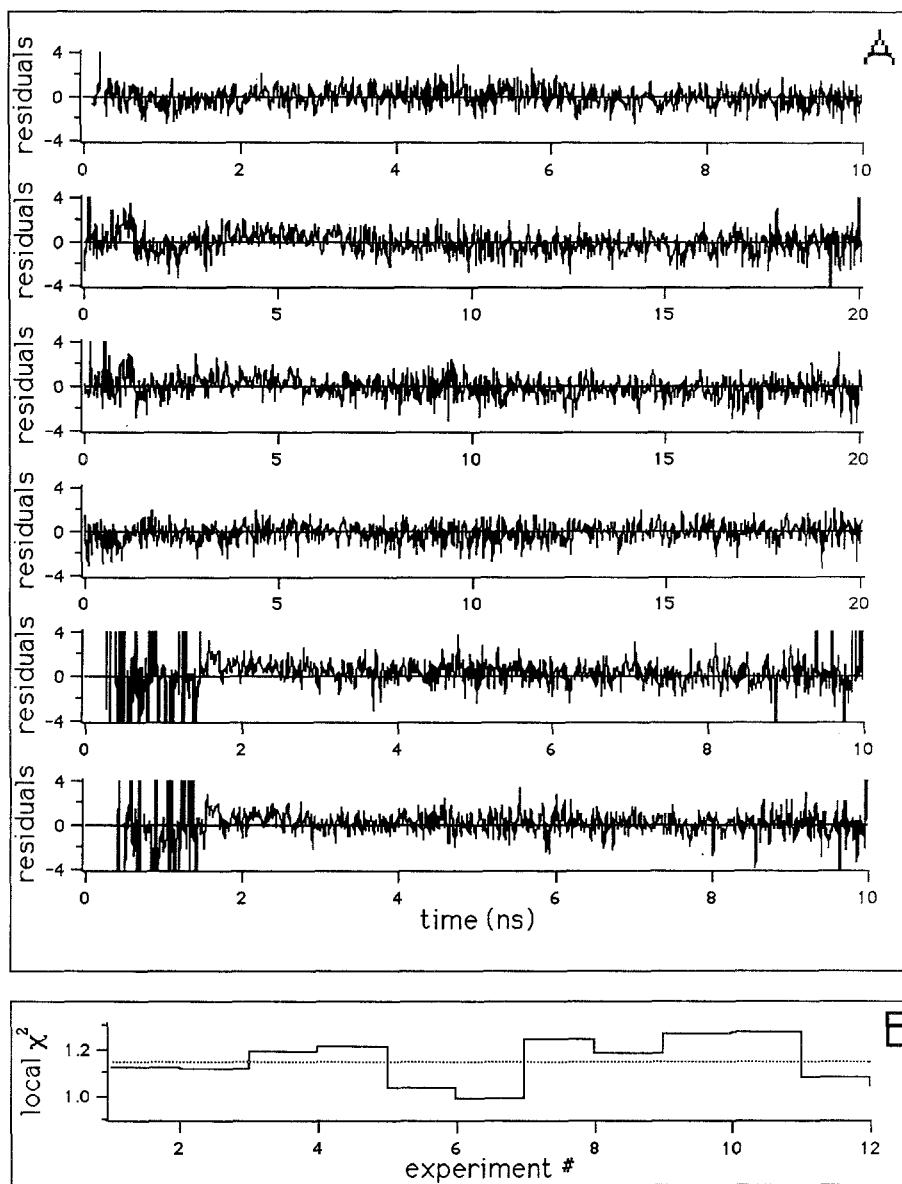


**Fig. 2.** Criteria of fit of fluorescence anisotropy data surface of electron transferring flavoprotein. (A) Weighted residuals of anisotropy decays. From top to bottom:  $\lambda_{\text{ex}}, 514.5 \text{ nm}$ ;  $\lambda_{\text{em}}, 539 \text{ nm}$  (laser);  $\lambda_{\text{ex}}, 457.9 \text{ nm}$ ;  $\lambda_{\text{em}}, 501 \text{ nm}$  (laser);  $\lambda_{\text{ex}}, 457.9 \text{ nm}$ ;  $\lambda_{\text{em}}, 548 \text{ nm}$  (laser);  $\lambda_{\text{ex}}, 457.9 \text{ nm}$ ;  $\lambda_{\text{em}}, 569 \text{ nm}$  (laser);  $\lambda_{\text{ex}}, 435 \text{ nm}$ ;  $\lambda_{\text{em}}, 460 \text{ nm}$  (synchrotron);  $\lambda_{\text{ex}}, 445 \text{ nm}$ ;  $\lambda_{\text{em}}, 470 \text{ nm}$  (synchrotron). B: Cityscape plot of local  $\chi^2$  of parallel and perpendicular components of the fluorescence decays. Local  $\chi^2$  is represented by a solid line and the global  $\chi^2$  by a broken line.

intermolecular separation between the centers of the isoalloxazines of  $21 \pm 2 \text{ \AA}$ .

If the decrease in the fundamental anisotropy as observed for the isoalloxazines in ETF is due to picosecond reorientational motion, an upper and lower limit of the intermolecular distance can be estimated with the  $\kappa^2$ -contour plots of Dale *et al.* [8]. From Eqs. (5) and

(6) the transfer and axial depolarization factors can be readily calculated to be 0.60 and 0.88, respectively. The contour plot in Fig. 6 in Ref. 8 was then used to estimate the upper (3.2) and lower (0.1) boundaries of  $\kappa^2$ . By taking into account the uncertainty in the transfer correlation time, we obtained a distance of 12–23  $\text{\AA}$  for the FADs in ETF.

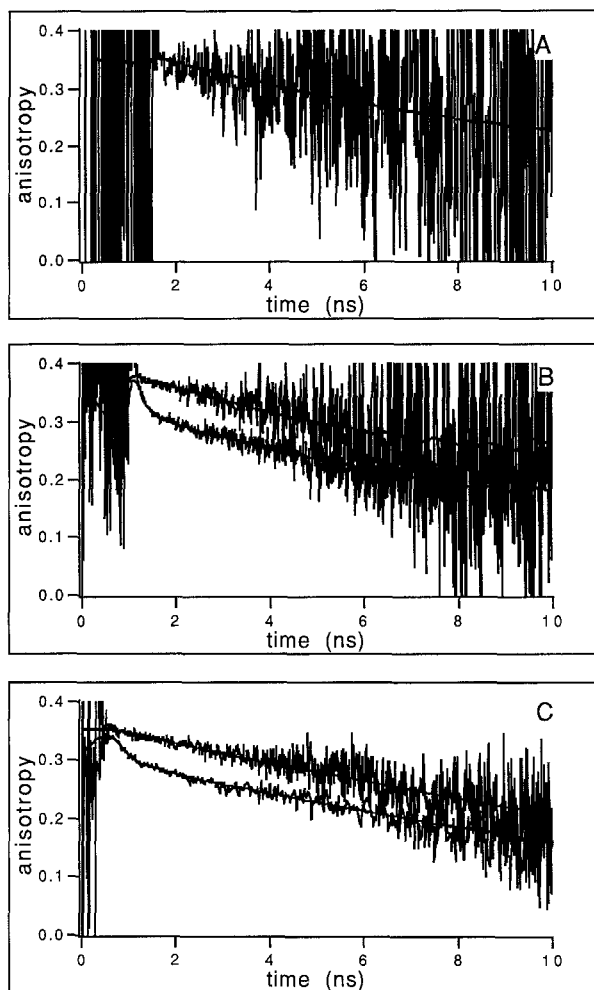


**Fig. 3.** Experimental and fitted anisotropy decays of electron transferring flavoprotein. (A) Blue-edge excited (445 nm) and detected (470 nm) (synchrotron). (B) Main-band (458 nm) and red-edge (515 nm) excited and detected (550–570 nm) as obtained by synchrotron excitation. (C) Similar to B, but with laser excitation.

## DISCUSSION

To our knowledge, this is the first report of failure of energy transfer as observed at the blue edge of the fluorescence emission spectrum of a binary homo-transfer system. Possible interference of the presence of a trace amount of 8-OH-FAD can be discarded on the basis of two criteria. First, upon 515-nm excitation, 8-OH-FAD would be excited in the main absorption band, and back transfer to FAD (or 8-OH-FAD) leading to depolarization can still take place because there is substantial spectral overlap between emission of 8-OH-FAD and absorption of FAD [19]. Such an effect is not observed (Fig. 3, Table III). Second, upon excitation at 445 and

detection at 470 nm, FAD is almost exclusively monitored, and under these conditions energy transfer indeed is not detected.

Both the red-edge excited and the blue-edge detected fluorescence anisotropy decay of ETF show that the depolarization of fluorescence upon main-band excitation and detection is caused by homo-energy transfer between the FAD cofactors together with protein tumbling. Red-edge and blue-edge failure of energy transfer will take place only in a system with inhomogeneously broadened spectra and a dipolar relaxation time much longer than the average fluorescence lifetime [9–11]. Consequently, the chromophores must then be located in an effectively rigid environment (on the time scale of fluorescence emission) with multiple conformations as sustained by the nonhomogeneous fluorescence decay.

The anisotropy decays as obtained from edge spectroscopy did not exhibit a short relaxation process that could be ascribed to restricted reorientational motion of the flavins, in agreement with the above-presented “solid-state” model of the active site of the protein. It is still possible that restricted reorientation of the flavins takes place on a time scale which is not resolvable by our experimental setup. The value of the initial anisotropy as obtained from the global analysis of the data surface was indeed lower (0.35) than the expected fundamental anisotropy (0.4). This discrepancy can be explained by high-frequency “rattling in a cage” of the isoalloxazines. It is, however, more probable that the absorption and emission transition moments in isoalloxazines do not coincide as the steady-state fluorescence anisotropy of flavins entrapped in rigid media do not exhibit the fundamental anisotropy of 0.4, but a value close to that found for the initial anisotropy of ETF [5]. Unfortunately, only an upper limit of the interflavin distance in ETF can be calculated in that instance. The angular parameters determined from the analysis of the experiments are highly accurate as demonstrated by a similar study of a double FAD-containing enzyme with a known crystal structure [12]. When the flavins undergo fast restricted motion, in addition to homo-transfer, the spread in the calculated distance is narrowed down considerably. This effect has been shown to occur in the biflavinyl-containing cytochrome P450 reductase, for which the three-dimensional structure is not yet known [5].

Concluding, it can be stated that a combination of edge spectroscopy and time-resolved fluorescence anisotropy adds an extra dimension to fluorescence depolarization methods. Both structural and dynamic information can be retrieved from the analysis of such a fluorescence anisotropy data surface.

**Table IV.** Fluorescence Anisotropy Decay Parameters of ETF as Obtained by Synchrotron Excitation<sup>a</sup>

Excitation and detection wavelength		Value of parameter			
$\lambda_{\text{ex}}$ (nm)	$\lambda_{\text{em}}$ (nm)	$\beta_1$	$\beta_2$	$\phi_p$ (ns)	$\phi_T$ (ns)
450 (S)	569	0.0646 (0.057–0.075)	0.315 (0.305–0.322)	12.5 (10.5–17.3)	0.141 (0.08–0.28)
515 (S)	569	"	"	"	98.9

<sup>a</sup>See Table III, footnotes a–c, for explanation of symbols.**ACKNOWLEDGMENTS**

The use of the Synchrotron Radiation Source in Daresbury (England) was made possible by The Netherlands Organisation of Scientific Research (NWO) in connection with the agreement between SERC and NWO.

**REFERENCES**

- H. L. Brockman and W. A. Wood (1975) *J. Bacteriol.* **124**, 1447–1453.
- C. D. Whitfield and S. G. Mayhew (1974) *J. Biol. Chem.* **249**, 2801–2810.
- F. Tanaka and N. Mataga (1979) *Photochem. Photobiol.* **29**, 1091–1097.
- P. I. H. Bastiaens, P. J. M. Bonants, A. van Hoek, F. Müller, and A. J. W. G. Visser (1988) *Proc. SPIE* **909**, 257–262.
- P. I. H. Bastiaens, P. J. M. Bonants, F. Müller, and A. J. W. G. Visser (1989) *Biochemistry* **28**, 8416–8425.
- A. J. W. G. Visser, J. S. Santema, and A. van Hoek (1983) *Photobiochem. Photobiophys.* **6**, 47–55.
- T. Förster (1948) *Ann. Physik.* **2**, 55–75.
- R. E. Dale, J. Eisinger, and W. E. Blumberg (1979) *Biophys. J.* **26**, 161–194.
- I. M. Gullis and A. I. Komjak (1977) *J. Appl. Spectrosc. (U.S.S.R.)* **27**, 841–845.
- I. M. Gullis and A. I. Komjak (1980) *J. Appl. Spectrosc. (U.S.S.R.)* **32**, 897–902.
- A. P. Demchenko (1987) *Ultraviolet Spectroscopy of Proteins*, Springer-Verlag, Berlin, pp. 183–197.
- P. I. H. Bastiaens, A. van Hoek, J. Benen, and A. J. W. G. Visser (1991) in preparation
- G. Weber (1960) *Biochem. J.* **75**, 335–345.
- G. Weber and M. Shinitzky (1970) *Proc. Natl. Acad. Sci. USA* **65**, 823–830.
- N. A. Nemkovich, A. N. Rubinov, and U. I. Tomin (1988) Preprint, N525, N526 of the Institute of Physics of BSSR, Academy of Science.
- J. R. Knutson, J. M. Beechem, and L. Brand (1983) *Chem. Phys. Lett.* **102**, 501–507.
- J. M. Beechem and E. Gratton (1988) *Proc SPIE*, **909**, 70–81.
- J. M. Beechem, E. Gratton, M. Ameloot, J. R. Knutson, and L. Brand (1991) in J. R. Lakowicz (Ed.), *Topics in Fluorescence Spectroscopy* (Vol. 2), *Principles*, Plenum Press, New York (in press).
- S. Ghisla and S. G. Mayhew (1973) *J. Biol. Chem.* **248**, 6568–6570.
- D. V. O' Connor and D. Philips (1984) *Time-Correlated Single-Photon Counting*, Academic Press, London.
- A. van Hoek and A. J. W. G. Visser (1981) *Rev. Sci. Instrum.* **52**, 1199–1205.
- I. H. Munro, D. Shaw, and M. M. Martin (1985) *Anal. Instrum.* **14**, 465–482.
- K. Vos, A. van Hoek, and A. J. W. G. Visser (1987) *Eur. J. Biochem.* **165**, 55–63.
- A. Szabo (1984) *J. Chem. Phys.* **81**, 150–167.
- M. D. Barkley, A. Kowalczyk, and L. Brand (1981) *J. Chem. Phys.* **75**, 3581–3593.
- P. R. Bevington (1969) *Data Reduction and Error Analysis for the Physical Sciences*, McGraw-Hill, New York.
- A. J. W. G. Visser and F. Müller (1979) *Helv. Chim. Acta.* **62**, 593–608.
- I. Z. Steinberg (1971) *Annu. Rev. Biochem.* **40**, 83–114.
- J. R. Lakowicz (1983) *Principles of Fluorescence Spectroscopy*, Plenum Press, New York, pp. 303–305.